AIAA-96-0932

AIRCRAFT AERODYNAMIC EFFECTS DUE TO LARGE DROPLET ICE ACCRETIONS

M.B. Bragg
University of Illinois at Urbana-Champaign
Urbana, IL

34th Aerospace Sciences Meeting & Exhibit
January 15-18, 1996 / Reno, NV

AICRAFT AERODYNAMIC EFFECTS DUE TO LARGE DROPLET ICE ACCRETIONS

M. B. Bragg*
University of Illinois at Urbana-Champaign

ABSTRACT

The effect of large-droplet ice accretion on aircraft control and in particular lateral control is examined. Supercooled large droplet icing conditions can result in the formation of a ridge of ice aft of the upper surface boot. By comparing this ice shape to data acquired with a spanwise protuberance on a different airfoil, it is clear that a ridge of ice aft of the boot can lead to large losses in lift, increases in drag and changes in the pitching moment. This effect is most likely due to the formation of a large separation bubble aft of the ice accretion which grows with angle of attack and eventually fails to reattach, leading to premature airfoil stall. The bubble alters the pressure distribution about the airfoil resulting in a more trailing edge up (negative) hinge moment on the aileron and the resulting change in aileron stick force. This can lead to aileron hinge moment reversal and aileron snatch. In aileron snatch the hinge moments are altered to the extent that the aileron is pulled up by the low pressure over the upper surface of the aileron with sufficient force to induce a rapid roll if a large stick force is not immediately exerted to oppose it. There is evidence in the literature which shows that similar lateral control problems are possible with other types of ice accretions and airfoil types.

INTRODUCTION

It is well known that ice formation on aircraft surfaces can lead to deterioration of performance and handling characteristics. Loss of aircraft control, where structural ice accretion has been identified as a probable cause, has in some cases been attributed to the presence of supercooled large droplets (SLD) in the atmosphere.

Supercooled large drops (SLD) can form in several ways[1]. One way for the SLD to form is through the melting of snow as it falls through a warm layer of air. This can happen when a warm frontal layer penetrates through a cold layer of air, causing a temperature inversion with increasing altitude, Fig. 1. Clouds above the warm layer produce snow which melts while falling through the warm layer and forms drizzle or rain drops. As the drops continue to fall, they enter the colder air layer again and are not likely to freeze again until they impact an object. If the lower cold air layer is at a sufficiently low temperature, the drops may freeze in the air to form ice pellets.

SLD may also form from smaller cloud drops. Droplets falling at different speeds can collide with one another and coalesce to form larger drops, Fig. 2. The presence of wind shear and a stable thermodynamic profile near stratiform cloud tops has been attributed to enhanced mixing and increased drop size[1].

On October 31 1994, an ATR-72 commuter aircraft crashed after loss of control in icing conditions. The meteorological conditions in the region of aircraft's holding pattern just prior to the accident suggested the possibility of the development of supercooled drizzle[1]. Supercooled large droplets, in the range of 30-400 μm, have been encountered by research aircraft while collecting data on effects of ice accretion on aircraft performance[2-5]. The reduction in the aircraft performance was reported to be unusually large during this encounter. Measured drag increased by as much as a factor of two, while the lift decreased more than 60%[5]. In another flight test in icing conditions, the worst icing encounter was identified as freezing rain[6]. The formation of ice during that encounter was described as ridges downstream of the leading edge on the wing and tails. Other accidents have also occurred due to the loss of aircraft control in conditions where SLD may have been present[7].

Recent flight tests behind a tanker at Edwards Air Force Base to reproduce large droplet icing conditions caused the formation of ice ridges downstream of the de-icing boots which might have led to an uncommanded roll[8]. The presence of ice ahead of the ailerons on the wing leading edge have been attributed to substantial reduction in aileron control[9] (Figure 3). Uncommanded roll due to aileron ineffectiveness was identified as the

* Professor, Department of Aeronautical and Astronautical Engineering, Associate Fellow, AIAA.

probable cause of three separate An-12 aircraft accidents[10]. The formation of ice upstream of the ailerons was cited as the cause of flow separation on the wing which led to the reversal of aileron hinge moment.

The phenomenon of ice accretion leading to reduced aircraft control has been observed and documented for over 50 years. This has primarily been for Appendix C type icing clouds, but there is also evidence of large droplet icing also causing control problems. It is the intent of this paper to identify the underlying aerodynamic causes of reduced aircraft control due to large droplet ice accretions. However, most of the discussion will also apply to leading-edge ice accretions resulting from smaller supercooled droplets as well.

DISCUSSION

Ice Accretion

It is well known that as the droplet size increases, the droplet inertia increases, and droplet impingement moves further back on the airfoil surface. The combination of this, with temperatures near freezing, leads to ice accretion shapes which are only now beginning to be studied. As part of the ATR 72 accident investigation, the Air Force icing tanker was modified to produce large droplets in the 100-200 micron range. A typical ice accretion obtained on the ATR-72 test aircraft[11] is shown in Fig. 4. This ice accretion was formed at 180 KIAS, T = -2 C, MVD = 140 microns, LWC = 0.3 g/m^3 for 17.5 minutes with the flaps at 0 degrees. Here a ridge of ice is seen which formed aft of the de-icer boot, between 7 and 9 percent chord on the upper surface with a small ridge also formed on the lower surface. The ridge was found to be jagged in most cases and discontinuous in the spanwise direction. The maximum ridge height on the upper surface for the conditions tested was 0.75 inches and 0.5 inches on the lower surface. When ice was accreted with the flaps at 15 degrees, the ice accretion moved back on the airfoil upper surface with a ridge at 9% and accretion to 14%. This occurred due to the reduction in angle of attack required with flaps to maintain the same lift coefficient. Therefore, the result was more exposure of the upper surface to the icing cloud and impingement further back on the upper surface. Similar results have been obtained in the Icing Research Tunnel at NASA Lewis[12].

Aerodynamics of Large Droplet Accretions

To the author's knowledge, no experimental studies have been made to date on the aerodynamics of airfoils with these types of ice accretions. However, information can be drawn from a few prior studies to help understand what the aerodynamic effect of a large droplet accretion may be. In 1932 Jacobs[13] conducted wind tunnel tests on an NACA 0012 airfoil to determine the effect of spanwise protuberances on the aerodynamic characteristics. The experiments were conducted at Re = 3.1x10^6 with the purpose of documenting the effects of "small projecting objects such as fittings, tubes, wires, rivet heads, lap joints, butt straps, filler caps, inspection plates and many other projections" on the performance of the airfoil. The airfoil with the locations of the spanwise protuberances are shown in Fig. 5. The protuberances were duralumin sheets placed in slots in the wing, one at a time, which acted as forward and aft facing steps. The chordwise width of the protuberance was not reported, but heights of k/c = 0.0004, 0.001, 0.002, 0.005 and 0.0125 were tested. For the large droplet case, the ice accretion shown in Fig. 4 occurs between the x/c=0.05 and 0.15 protuberances tested by Jacobs. The maximum height of 3/4 inch seen in the large-droplet tanker test ice accretions has a k/c = 0.0106 based on an airfoil chord at the aileron midspan location of 5.9 ft. At the conditions of the tanker test, this section would have been operating at a chord Reynolds number of 8.95x10^6. The NACA test was conducted at sufficiently high Reynolds number that with these roughness heights, which are very large compared to the local boundary-layer thickness, the simulation should be representative of the behavior of airfoils with large-droplet ice accretions at full-scale commuter aircraft Reynolds numbers.

In Fig. 6 section lift, drag and pitching moment results are shown for the NACA 0012 airfoil with 4 different roughness height protuberances all at x/c=0.05 on the airfoil upper surface. For protuberances of k/c=0.001 and 0.002 the effect on lift is a slight reduction in lift curve slope and a sizable reduction in maximum lift. For k/c=0.005 the lift curve is further reduced, but here only a local maximum in lift is seen with the lift continuing to increase as angle of attack is increased. This trend is continued for k/c=0.0125 with no maximum or local maximum seen in lift. The lift breaks sharply around α = 6°, becomes almost constant until α = 12°, where it increases again at a reduced, but linear, lift curve slope. The drag polar in Fig. 6 b) shows that this loss in lift is accompanied by a large increase in drag, especially for the 2 largest protuberance sizes. The pitching moment data in Fig. 6 c) shows a much more negative, nose down, pitching moment for the k/c=0.0125 case starting at α = 6° where the lift curve breaks. The effect on pitching moment is much less for the smaller roughness cases where the primary effect is a reduced maximum lift at almost the same stall angle. For the large roughness, this change in moment is indicative of a large change in pressure distribution on the airfoil which accompanies the loss in lift. A NACA 0012 airfoil has most of its lift on the forward part of the airfoil. A loss in lift on the forward part of the airfoil would account for the large increase in nose-down moment.

The data of Jacobs[13] can also be used to determine the effect of protuberance location on lift loss. Figure 7 shows the measured lift on the airfoil with the

k/c=0.0125 protuberance at 5 different surface locations. For angles of attack in the 8 to 16 degree range the largest lift loss is due to the protuberance at the x/c=0.05 location on the upper surface. The lift with the protuberance at x/c= 0. and 0.15 is higher at all angles in this range. With the protuberance at the leading edge, a very gentle stall is seen at a reduced angle from the clean case with a large reduction in maximum lift. The x/c=0.15 case behaves much like the x/c=0.05 case described earlier where around $\alpha = 6°$ a large reduction in lift curve slope is observed. A protuberance on the lower surface had almost no effect on the airfoil lift. Wenzinger and Bowen[14] tested round and flat spoilers on the upper surface of a 3-D wing in the Langley 19-foot wind tunnel. The effect on lift and drag was very similar to that seen by Jacobs. Wenzinger and Bowen concluded that the largest lift loss came from the spoiler placed on the upper surface between 5 and 20% chord. Therefore, for the large droplet ice accretion case, the observed upper surface ice accretion locations of between 7 and 9% chord are in the most sensitive region on the airfoil for loss in lift due to a protuberance.

Figure 8 provides some information as to the effect of the shape of the cross-section of the protuberance on the lift loss[13]. Jacobs faired some of the protuberances using plaster-of-Paris to make them approximately 1/2 airfoil shape. The effect on the lift for the k/c=0.005 protuberance at x/c=0.05 on the upper surface is quite dramatic. Here the maximum lift is increased from 0.82 to 1.27 by fairing the protuberance as compared to the clean airfoil maximum lift of 1.52. The reduction in the drag coefficient is also dramatic. These data demonstrate that the shape of the protuberance has a significant effect on the resulting aerodynamic penalty. Again, similar results were reported by Wenzinger and Bowen[14] showing flat spoilers more effective than round spoilers. Jacobs does not report the exact shape of the faired or original protuberance, but the large-droplet ice accretion will most likely fall some place between these two shapes.

The lift performance of the airfoil with the large protuberance at x/c=0.05 and 0.15 as seen in Fig. 8 is very similar to that seen on an airfoil which experiences thin airfoil stall[15,16]. In thin airfoil stall, a separation bubble forms from the airfoil leading edge and grows in chordwise extent as the angle of attack is increased. When the bubble fails to reattach, or reaches the trailing edge, the airfoil stalls. In most sections a discontinuity can be seen in the lift versus angle of attack curve at the angle of attack where the bubble forms and begins to grow, Fig. 9. In some sections, the discontinuity can be so large due to the sudden and rapid growth of the bubble as to actually cause a local maximum in lift, followed by increased lift as α is increased further. This type of behavior is seen in Fig. 8 in the unfaired protuberance data. The k/c=0.0125 protuberance caused a discontinuity in the lift at $\alpha = 6°$ when placed at x/c=0.05 or 0.15, Fig. 7. This is probably due to the thin airfoil-like behavior of the separation due to the protuberance. As the angle of attack reaches 6°, the separation bubble caused by the protuberance grows rapidly, causing the abrupt change in lift performance at this angle. Above this angle of attack, the bubble grows more slowly with angle of attack. This slow growth effectively decambers the airfoil reducing the lift curve slope. This decambering due to the bubble reduces the suction peak pressure resulting in the more negative, nose down, pitching moment which was measured, Fig. 6.

Thin airfoil stall behavior has been observed before on an airfoil with a simulated leading-edge ice accretion. Bragg et. al.[17,18] tested simulated gaze ice accretions on a NACA 0012 airfoil. The airfoil experienced a large separation bubble aft of the upper surface horn which grew in chordwise extent as the angle of attack was increased, Fig. 10. At 6 degrees and above the flow was very unsteady and the bubble failed to reattach in a time averaged sense. This corresponds to the measured lift coefficient for the clean and iced airfoil shown in Fig. 11. The iced airfoil has a slightly reduced lift curve slope at low angles, but the most dramatic effect is the large break in the lift above 5 degrees. This is where the bubble grows rapidly and eventually failed to reattach to the surface. No measurements were taken above $\alpha = 9°$ due to the large unsteady loads on the model. It is possible that the lift would have increased as α was further increased. This leading-edge ice accretion, simulating a conventional Appendix C cloud encounter, is indeed behaving much like the cases with a large protuberance near the leading edge measured by Jacobs[13]. It also has all the characteristics of a very severe thin airfoil stall. The pressure distribution confirms that this is a thin airfoil stall. In Fig. 12 the pressure distribution[17] for the clean airfoil is compared to the simulated ice case at three angles of attack. At $\alpha = 4°$ the spike in Cp seen on the leading edge of the clean airfoil is replace by a region of constant pressure. This constant pressure region is due to the separation bubble aft of the ice horn. As the angle of attack increases, the constant pressure region grows as the bubble grows in length. At $\alpha = 8°$ the separation bubble fails to reattach and the character of the pressure distribution changes. Note the almost constant pressure region extends to x/c = 0.40 with only a small amount of pressure recovery occurring from this location to the trailing edge (i.e. the Cp at the trailing edge is much more negative indicating a lower pressure). The effect of this large change in trailing-edge pressure on an aileron will be discussed later. These pressure distributions are very similar to those on an airfoil with thin airfoil stall, such as in Fig. 9.

In this section the aerodynamics of an airfoil with a large-droplet ice accretion have been examined using prior studies on airfoils with protuberances, thin airfoil stall and a large leading-edge ice accretion. Although no aerodynamic data are available on an airfoil with a large-

droplet ice accretion, it is very likely that it behaves as shown in Fig. 13. The ice accretion causes a separation bubble to form aft of the ice accretion. At low angles of attack the effect is a reduction in lift curve slope and a small change in zero lift angle of attack. In some angle of attack range depending on the size and location of the ice accretion, the separation grows rapidly causing a large change in lift curve slope and maybe a local maximum in lift coefficient. Further increase in α sees the lift increase again, but at a much reduced lift curve slope. Similar aerodynamic effects were seen on an airfoil with a leading-edge ice accretion. There are not enough data at this time to compare the aerodynamic effects of leading-edge and large-droplet ice accretions. However, based on Jacobs' work, it may be that ice accretions on the upper surface, back slightly from the leading edge produce larger aerodynamic penalties for the same ice accretion height.

Aerodynamic Hinge Moments

Perhaps the most dangerous effect of ice accretion on aircraft is the change in the pilot's ability to control the aircraft. Not only are the effectiveness of the controls crucial, but also the feedback the pilot receives through the hinge moments and stick forces. In this section the basics of aileron control of an aircraft will be reviewed, followed by a discussion of how ice accretion on the wing can affect the aileron control. The discussion deals only with the aileron, but most of the discussion could just as well be about an elevator or rudder control system.

Background

Ailerons are used to provide the pilot with a means of lateral control of the aircraft. Ailerons are typically plain flaps mounted on the trailing-edge sections of the outer wing. A plain flap is simply some portion of the airfoil trailing-edge (typically .15c to .20c) that is hinged about a point within the contour. If no gap is present as a result of the hinge, deflecting the flap essentially changes the camber of the airfoil. For a given section angle of attack, a plain flap of 0.20c is capable of producing increments in sectional lift ranging up to about 1.0.[19] Deflection of the flap also increases the $C_{\ell_{max}}$ of the section. When used as ailerons, the plain flaps on each side of the wing are deflected asymmetrically. This asymmetric deflection alters the spanwise load distribution across the wing such that a rolling moment is generated. A diagram showing the spanwise loading of a wing with and without deflected ailerons is given in Fig. 14. Ailerons are usually designed to provide enough lateral control to allow sufficient rolling moment at low speeds to counter asymmetric gusts and also to provide a sufficiently high roll rate at high speeds.[20] One of the most important aspects of aileron and control surface design are the forces that the pilot must overcome at his cockpit controls and which also provide a sense of "feel" to the aircraft.

These forces are generated by the pressure distribution over the aileron or plain flap itself. The pressure distribution over the aileron creates a moment about the control surface hinge referred to as a hinge moment. If the aileron is free to float, or move without restriction, it will rotate up or down depending upon the pressure distribution over the aileron. For most cases, the low pressure created over the upper surface of the wing will cause the aileron to want to rotate up. The aileron control forces and hinge moments are somewhat complicated due to the fact that there are two surfaces, one moving up and the other moving down. This is further complicated by the fact that as the aircraft rolls, a new lift distribution will be created that is a function of the rolling velocity and opposes the rolling moment due to the aileron deflection. This opposing moment is a result of a change in the effective angle of attack for sections along the wing due to the rolling velocity. For the purpose of the discussion of hinge moments, however, the hinge moment produced by the deflection of a plain flap, which in this case is assumed to be a single aileron, provides the clearest and simplest approach.

There are two major variables which control the pressure distribution over the aileron. These are the angle of attack of the section and the deflection angle of the aileron. Changes in both the angle of attack of the section and deflection angle of the aileron affect the pressure distribution over the entire airfoil and as a result change the magnitude of the hinge moment. The magnitude of the hinge moment for any combination of sectional angle of attack and aileron deflection angle can be developed from a linear summation of the effects of each. Typical pressure distributions for a section at zero degrees angle of attack, but with varying aileron deflection angles, along with pressure distributions resulting simply from changes in angle of attack are shown in Fig. 15. The suction created over the upper surface of the aileron as the aileron is deflected downward can be represented as the reaction R acting through the centroid of the pressure area and thereby creating the hinge moment about the hinge line. The hinge moments are nondimensionalized by the area of the control surface and by the root mean square of the chord of the control surface aft of the hinge line. From the summation of the effects shown in Fig. 3, the aileron hinge moment coefficient, C_{h_a}, can be expressed as:

$$C_{h_a} = C_{h\alpha}\alpha + C_{h\delta}\delta_a + C_{h0}$$

where $C_{h\alpha}$ and $C_{h\delta}$ represent the change in hinge moment due to angle of attack and aileron deflection, respectively. C_{h_0} is a general term to account for residual hinge moment due to cambered surfaces. The term d_a

refers to the total aileron angle in degrees and is equal to the sum of the deflection of the up aileron and the deflection of the down aileron. A plot showing the typical change in aileron hinge moment with angle of attack and deflection d_a is given in Fig. 16. Aileron stick force is considered positive for a force towards the pilots right and hinge moments are positive due to trailing-edge down aerodynamic moments. The hinge moments of ailerons used in actual practice are usually quite non-linear, and differential gearing of the ailerons is often used to give the up-going aileron more deflection than the down-going aileron[20]. The simple linear analysis presented above, however, provides a basic introduction to ailerons and aileron hinge moments required for latter discussions of the effect of ice on roll rates and overall aircraft feel.

Another area needing brief review is that of the aerodynamics associated with a typical clean wing stall. A review of clean wing stall characteristics is important as they play a large roll in aileron effectiveness and aircraft roll and controllability during stall. Recall for a finite wing with an elliptic circulation distribution that the sectional lift coefficient is constant along the span. As a result, all sections will reach stall at essentially the same angle of attack. For a rectangular wing, the spanwise load distribution shows that sectional lift coefficients are greatest near the root, implying initial boundary-layer separation and stall will begin near the root and progress outwards along the span as the angle of attack is increased. By tapering the rectangular planform, the span load distribution can be made to approximate that of an elliptic distribution. Since the distribution is not completely elliptic, however, the sectional lift coefficient is not constant along the span. Instead, as taper ratio increases, the maximum sectional lift coefficient moves out along the span. For a triangular wing, taper ratio of zero, sectional lift coefficients are greatest at the tip and separation and stall will begin at the tip. Therefore, for a moderately tapered unswept planform sectional lift coefficients and stall will begin at some point along the midspan. This is somewhat troubling as the ailerons used to provide lateral control are located near the midspan. A desirable wing stall pattern is one that begins near the root. Separation and unsteady flow structures shed from the initial stall pattern near the root will be felt by the pilot as they pass over the tail. More importantly, however, lateral control of the aircraft will be maintained through the initial stall as the outboard sections containing the ailerons are still attached. In order to prevent the stall pattern from beginning in the region of the ailerons, the wing may be given a geometric twist, or washout, to decrease the local angles of attack near the tip ensuring that the root sections will stall first.[21] The effect of premature stall due to ice accretion, however, can significantly alter the wing's stall pattern and the pilots ability to control the aircraft during stall.

Effect of Ice on Hinge Moments

The effect of ice accretion on lateral control effectiveness, lateral control feel, and lateral controllability can be quite pronounced. These serious effects are the result of flow separation due to the presence of the ice accretion. When the amount of flow separation is small, usually at low angle of attack or small ice accretions, the effect on aircraft control is also small. However, tests (see Figs. 6, 7, 8 and 11) show that the break in the lift curve, and therefore the onset of large regions of separated flow, begins at lower angles of attack with simulated ice on the airfoil. This early separation leads to a larger suction force on the top of the aileron and therefore a more negative aileron hinge moment than would exist on the uniced airfoil. Compare the pressure distributions shown in Fig. 12 with and without simulated ice. The lift just ahead of the trailing edge is much larger on the iced airfoil due to the separation induced by the ice shape. As a result, there is a large increase in trailing-edge up (negative) hinge moment. In Fig. 17 pressure distributions from three airfoils[15] have been integrated to yield the aileron hinge moment for a 20% chord plain flap at zero degrees flap deflection. The NACA 63-018 airfoil has a gradual trailing-edge stall, while the NACA 64A006 and the double diamond airfoil (see also Fig. 9) both have thin airfoil stalls which are thought to be similar to that occurring on iced airfoils. Note that when the leading-edge separation bubble grows rapidly on the 64A006 and diamond airfoil at 6 and 11 degrees angle of attack, respectively, a large trailing-edge up hinge moment is generated. The trailing-edge stall airfoil which can be thought of as the uniced airfoil, has a much more gentle break in its C_h curve and at much higher angle of attack. Note also that the ice-induced upper surface separation will also greatly reduce the effectiveness of the aileron to produce a rolling moment. It may even be possible for the aileron control itself (not just the hinge moment) to reverse if positive aileron deflection causes the wing to stall prematurely and as a result the aircraft rolls in the opposite direction as intended. Figure 3, from reference 9, shows the measured rolling moment produced by full aileron deflection with and without leading-edge ice on a 3-D wing. At low lift coefficients, the aileron on the iced wing produced significantly less rolling moment and no control power was available above approximately a $C_L = 0.7$ where the iced wing reaches its maximum lift.

When ice has accreted on the wing leading edge ahead of the aileron, the possibility of aileron hinge moment reversal exists. Recall from Fig. 16, for a positive aileron deflection (trailing-edge down), the aileron hinge moment is negative. Physically, as the aileron is deflected down, acting as a plain flap, the pressure over the upper surface of the aileron decreases and the aileron wants to float upward. Conversely, if the aileron is deflected up, a comparatively higher pressure

exists over the upper surface of the aileron creating a more positive hinge moment forcing the aileron down. If, for the case of a large droplet ice accretion, a spanwise ridge is present on the upper surface of the airfoil in front of the aileron, an area of separated flow will exist downstream of the accretion. The size and extent of this region, or separation bubble, will grow with angle of attack (Fig. 13). As the angle of attack is increased, the separation bubble grows increasing the suction pressure on the top of the aileron. As the aileron is deflected up at this high angle of attack, a low pressure region still exists over the aileron due to the presence of the ice induced separation. This low pressure will cause a trailing edge up hinge moment about the aileron. This is opposite of what would normally happen for an upward aileron deflection as discussed above. As a result, the aileron hinge moment for the case where ice induced separation is present upstream of the aileron may produce a much less positive or even negative hinge moment for an upward deflected aileron. Since this hinge moment behavior is opposite of that observed for the clean wing at angle of attack, the condition is termed hinge moment reversal.

For cases where hinge moment reversal is present, the lateral control feel of the aircraft is very different. Consider a turn to the right. The pilot exerts a positive stick force moving the stick to the right which causes the right aileron up and the left aileron down. If hinge moment reversal is present on the right wing due to ice, the right aileron experiences a trailing edge up moment and thus the pilot's stick force required to make the turn is less. If the hinge moment reversal is severe, the pilot may actually have to apply a negative stick force (to the left) to hold the right aileron from being sucked up and increasing the bank angle. This severe case is known as "aileron snatch". So named because the stick force may be great enough to "snatch" the yoke or stick from the unsuspecting pilot as the aileron rotates upward.

A form of aileron snatch may provide a plausible explanation for the recent ATR 72 accident. Instead of the snatch occurring abruptly due to an unsteady aerodynamic effect, the snatch was effectively induced by the auto-pilot. As ice accreted on the aircraft, areas of separation were most likely present on the wing upper surface. With the auto-pilot engaged, small changes in the lateral control feel of the aircraft resulting from the accretion would be transparent to the pilot as the auto-pilot is unaware of changes in the lateral control forces. The auto-pilot merely senses attitude and rates and corrects accordingly. If the aileron hinge moment forces became to great, however, the auto-pilot would disengage as some maximum force level is approached. As the auto-pilot disengages, the strong low pressure region over one of the ailerons created by the ice induced separation would cause the aileron to rotate upwards violently. The aileron snatch has occurred as a result of the auto-pilot disengaging.

From the flight data recorder of the ATR 72 for flight 4184, 10 seconds prior to the auto-pilot disengaging, the aircraft was flying with 15 degrees of flap, slightly nose down, and in a slight 15 degree right hand bank[22]. With 15 degrees flaps and large droplet freezing drizzle, the Air Force icing tanker tests showed[11] that an ice accretion would form relatively far back on the chord with a ridge at x/c=9% and accretion to 14%. The ridge, downstream of the de-ice boots, was most likely discontinuous in the spanwise direction and more severe on the right wing than the left. At this point there might already be some aileron hinge moment reversal present due to the ice. Since the auto-pilot is engaged, however, the pilot is unaware of changes in the feel of the aircraft due to the ice or the aileron hinge moment reversal.

The pilot then retracts the flaps approximately 6 seconds before autopilot disconnect. As the flaps retract, the auto-pilot commands the aircraft to rotate to a higher angle of attack to maintain the same lift coefficient. As the aircraft rotates to a higher angle of attack, the areas of ice induced separation become larger, as quite possibly does the hinge moment reversal. At some point, either due to the growing forces resulting from the hinge moment reversal, or due to a large sudden increase in the aileron forces as a result of some unsteady separation or change in the ice induced bubble location and extent, the auto-pilot disengages. It is at this point where the aileron snatch scenario begins. After the auto-pilot disconnects, the right wing aileron rotates up violently. Having previously been on auto-pilot, as the system disconnects, the pilot does not have his hands on the controls. The aileron snatch has occurred as a result of the auto-pilot disconnect. After some finite amount of time (approximately 1.7 seconds after disconnect)[22] the pilot attempts to regain control. The aircraft has already rotated right wing down 70 degrees. Fighting the hinge moment reversal and snatch forces, the pilot attempts to right the aircraft with opposite aileron (left wing aileron up and right wing aileron down) to effect a roll to the left to level the aircraft. The aircraft comes back to 50 degrees right wing down. Shortly there after the aircraft rolls right again and the pilot cannot recover. The second roll might be a result of the opposite aileron deflection. As the pilot fights the hinge moment reversal and attempts to level the aircraft by commanding the right aileron down, the separation over the right aileron might increase dramatically due to the increased adverse pressure gradient created by the downward movement of the aileron itself. This increased separation over the right hand wing outboard section could cause this portion of the wing to stall, decreasing the loading on the right wing, and again causing the aircraft to roll to the right again. It should be noted that the above scenario is speculation based upon flight 4184 flight recorder data and a knowledge of ice induced airfoil and aircraft aerodynamics.

Modern Airfoils

Recent problems with commuter aircraft in icing conditions include the horizontal tail stall problem and the aileron control problem recently encountered by the ATR aircraft in probable large droplet icing conditions. In each case, the use of "modern" airfoils has been raised by some as being at least responsible in part for the problem. In this section the relationship of modern airfoils to these safety concerns is addressed.

The question of safety and "modern" airfoils goes back perhaps to the early 80's when laminar flow was rediscovered and its use on first homebuilt sport airplanes and later production airplanes was begun. Initially, the safety concern was well founded due to the use of laminar flow airfoils which suffered severe lift penalties when laminar flow was lost due to leading-edge contamination. The Voyager around the world aircraft was almost lost due to flight into light rain[23] early in its development. Longitudinal control was lost when the water on the canard surface caused a loss in lift as a result of early boundary-layer transition. Quickly, however, airfoil designers learned to design laminar flow airfoils with little lift loss due to early transition. Bragg and Gregorek[24] examined laminar flow airfoils with roughness and found that the percent decrease in performance was larger than for turbulent airfoils, but the absolute performance was in most cases better even with the same roughness.

What is a "modern" airfoil? For a commuter class aircraft a laminar flow airfoil would probably be considered modern. A computer designed and optimized airfoil for a particular mission might also be considered "modern" if it incorporated state-of-the art design methodologies and airfoil design practices. A precise definition of "modern" in this context is probably not possible. The ATR airfoil and its pressure distribution is shown in Fig. 18. along with that of a NACA 23015 airfoil. It is clear that the ATR airfoil is not a laminar flow section from the fact that the adverse pressure gradient starts near the leading edge on the upper surface. It is unclear whether this airfoil is indeed "modern" by our definition.

Regardless as to whether the ATR airfoil is "modern", it is clear that older NACA airfoils have effects due to ice accretions that can account for the suspected aileron control problem. The protuberance data reported by Jacobs[13] was acquired on a NACA 0012 and showed large lift losses due to spanwise protuberances in the 5 to 15% chord location. Research on a NACA 0012 airfoil with a leading edge ice accretion has shown similar effects[18] of a large separation bubble aft of the ice which leads to thin airfoil stall behavior and possible hinge moment reversal. Tests on other airfoils have shown similar results. Aircraft designed many years ago have experienced aileron control problems with ice. For example the measurements by Johnson[9] showing lack of aileron control power with leading-edge ice. Brumby[25] reports on a relatively small amount of ice on the wing of a commercial transport causing an accident on takeoff due to the loss of roll control. Several other loss of lateral control due to ice anecdotes have appeared in the literature as well.

There simply is not enough research to know if some airfoils are more susceptible to ice than others. Most research on the aerodynamic effect of ice on airfoils has been on older sections. This problem is now being addressed by NASA and more information should be available in the future. What is clear is that all airfoils are in some degree susceptible to a loss in performance due to the accretion of ice, and that this should be considered in the design and operation of the aircraft. Highly optimized systems may behave very poorly at off design points which were not considered in the design process. If wings or empenages are designed with highly optimized airfoils, icing should be considered in some fashion as a possible off-design condition.

SUMMARY

Large droplet icing conditions can result in the formation of a ridge of ice aft of the upper surface boot. By comparing this ice shape to data acquired with a spanwise protuberance on a different airfoil it is clear that this can lead to large losses in lift, increases in drag and changes in the pitching moment. This effect is most likely due to the formation of a large separation bubble aft of the ice accretion which grows with angle of attack and eventually fails to reattach leading to premature airfoil stall. This is very similar to the flowfield observed on airfoils with thin airfoil stall and leading-edge ice accretions which have similar lift performance.

The upper surface bubble alters the entire pressure distribution about the airfoil. In particular, it greatly reduces the surface pressure on the upper surface of any trailing edge flap (aileron or elevator). This results in a more trailing edge up (negative) hinge moment and a change in stick force. In a severe case on a wing, this could lead to aileron hinge moment reversal and aileron snatch. In aileron snatch the hinge moments are altered to the extent that the aileron is pulled up by the low pressure on the top with sufficient force to induce a rapid roll if a large stick force is not immediately exerted to oppose it. It is possible that this could have occurred in the recent ATR accident.

It has been speculated that this problem may be peculiar to aircraft with "modern" airfoils and only occur with large-droplet ice accretions. However, there is evidence in the literature which shows that similar lateral control problems are possible with other types of ice accretions and on older designed airfoils.

ACKNOWLEDGMENTS

Dr. Abdi Khodadoust provided much of the background information on supercooled large droplet icing and possible related aircraft accidents. Dr. Mike Kerho provided background information on aileron control systems and analyzed the effect of ice on aileron stick forces. Without their significant contributions, this paper would not have been possible. I would like to thank several other people who provide information for this paper. Mr. John Dow and Dr. Jim Riley of the FAA for their help in providing information on the ATR accident and other related matters. Mr. Tom Ratvasky and his coworkers at NASA for helping me understand the large droplet icing tanker and wind tunnel tests. ATR representatives provided data relating to their investigation of the accident. Dr. Marcia Politovich of NCAR helped me understand the meteorology of supercooled large droplet icing. Thanks to Mr. Shawn Noe and Mr. Chad Henze for their help with the figures.

REFERENCES

[1] Politovich et. al., "Meteorological Conditions Associated with the ATR-72 Aircraft Accident Near Roselawn, Indiana on 31 October 1994," *Proceedings of the International Icing Symposium '95*, Montreal, Canada, September 18-21, 1995, pp. 235-243.

[2] Cooper, W.A., Sand, W.R., Politovich. M.K., and Veal, D.L., "Effect of Icing on Performance of a Research Airplane," *Journal of Aircraft*, vol. 21, no. 9, September 1984, pp. 708-715.

[3] Sand, W.R., Cooper, W.A., Politovich. M.K., and Veal, D.L., "Icing Conditions Encountered by a Research Aircraft," *Journal of Climate and Applied Meteorology*, vol. 23, no. 10, October 1984, pp. 1427-1439.

[4] Politovich, M.K., "Response of Research Aircraft to Icing Conditions and Evaluation of Icing Severity Indices," accepted for publication in *Journal of Aircraft*, April 1995.

[5] Politovich, M.K., "Aircraft Icing Caused by Large Supercooled Drops," *Journal of Applied Meteorology*, vol. 28, no. 9, September 1989, pp. 856-868.

[6] Thoren, R.L., "Icing Flight Tests on the Lockheed P2V," ASME paper no. 48-SA-41, 1948.

[7] "Report on the Accident to Fokker F27 Friendship G-BMAU 2 NM West of East Midlands Airport on 18 January 1987," The Department of Transport, Air Accidents Investigation Branch, Aircraft Accident Report 7/88, HMSO, London, England.

[8] Dow Sr., John P., "Roll Upset in Severe Icing," Federal Aviation Administration - Aircraft Certification Service, September 1995.

[9] Johnson, C.L., "Wing Loading, Icing and Associated Aspects of Modern Transport Design," *Journal of the Aeronautical Sciences*, vol. 8, no. 2, December 1940, pp. 43-54.

[10] Teymourazov, R. and Kofman, V., "The Effect of Ice Accretion on the Wing and Stabilizer on Aircraft Performance," Unpublished Report, Interstate Aviation Committee, Moscow, Russia.

[11] National Transportation Safety Board, "Icing Tanker Test Factual Report", Docket No: SA-512, Exhibit No: 13B, DCA95MA001, Washington D.C., Feb. 16, 1995.

[12] Miller, D., Addy, H. and Ide, R., "A Study of Large Droplet Ice Accretions in the NASA Lewis IRT at Near Freezing Conditions", AIAA Paper 96-0934, Reno, NV, 1996.

[13] Jacobs, E. N., "Airfoil Section Characteristics as Affected by Protuberances", NACA Report N0. 446, 1932.

[14] Wenzinger, C.J. and Bowen, J.D., "Tests of Round and Flat Spoilers on a Tapered Wing in the NACA 19-Foot Wind Tunnel", NACA TN 801, March 1941.

[15] McCullough, G.B. and Gault, D.E., "Examples of Three Representative Types of Airfoil-Section Stall at Low Speeds", NACA TN 2502, Sept. 1951.

[16] Hoerner, S.F. and Borst, H.V., "Fluid-Dynamic Lift", Hoerner Fluid Dynamics, 1975, pp. 4-2 to 4-6.

[17] Bragg, M.B. and Coirier, W.J., "Aerodynamic Measurements of an Airfoil with Simulated Glaze Ice" AIAA Paper 86-0484, Jan. 1986.

[18] Bragg, M.B. and Spring, S.A., "An experimental Study of the Flow Field about an Airfoil with Glaze Ice", AIAA Paper 87-0100, Jan. 1987.

[19] Abbot, I. H., and Von Doenhoff, A. E., *Theory Of Wing Sections*, Dover Publications, Inc., New York, 1959.

[20] Perkins, C. D., and Hage, R. E., *Airplane Performance Stability and Control*, John Wiley and Sons, New York, 1949.

[21] Bertin, J. J., and Smith, M. L., *Aerodynamics For Engineers, 2nd Ed.*, Prentice Hall, New Jersey, 1989.

[22] "Freezing Drizzle Towards a Better Knowledge and a Better Prediction", published by ATR, Avions de Transport Regional, 1 Allee Piere Nadot, 31712 Blabnac, Cedex, France, Nov. 15, 1995.

[23] Bragg, M.B. and Gregorek, G.M., "Experimental Airfoil Performance with Vortex Generators", *Journal of Aircraft*, Vol. 24, No. 5, 1987, pp. 305-309.

[24] Bragg, M. B. and Gregorek, G. M., "Environmentally Induced Surface Roughness Effects on Laminar Flow Airfoils: Implications for Flight Safety", Paper No. AIAA-89-2049, AIAA/AHS/ASEE Aircraft Design, Systems and Operations Conference, Seattle, WA, July 1989.

[25] Brumby, R.E., "The Effect of Wing Contamination on Essential Flight Characteristics", Douglas paper no. 8127, presented at the SAE Aircraft Ground De-Icing Conference, Denver, Set. 20-22, 1988.

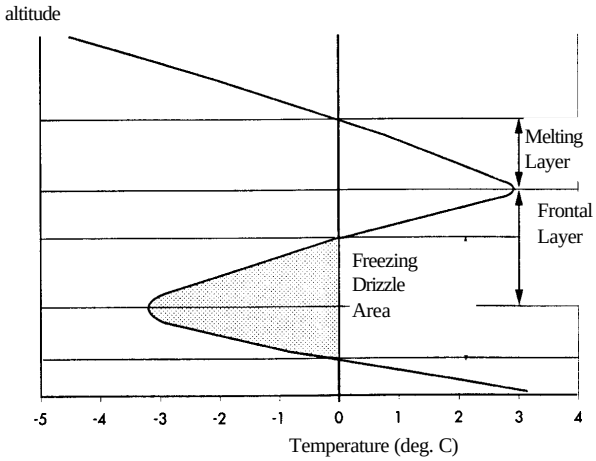

Figure 1. Presence of warm fronts produces regions prone to the formation of large supercooled drops[1].

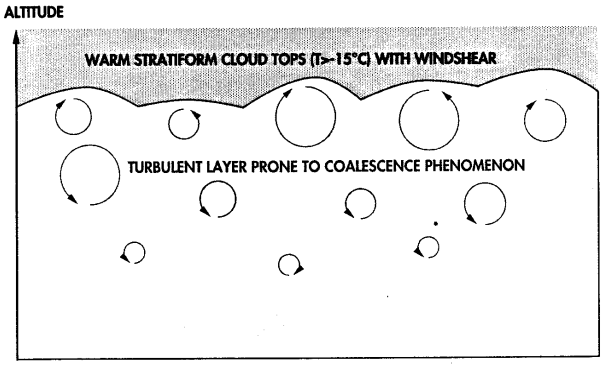

Figure 2. Coalescence as a major phenomena in the formation of supercooled drops[1].

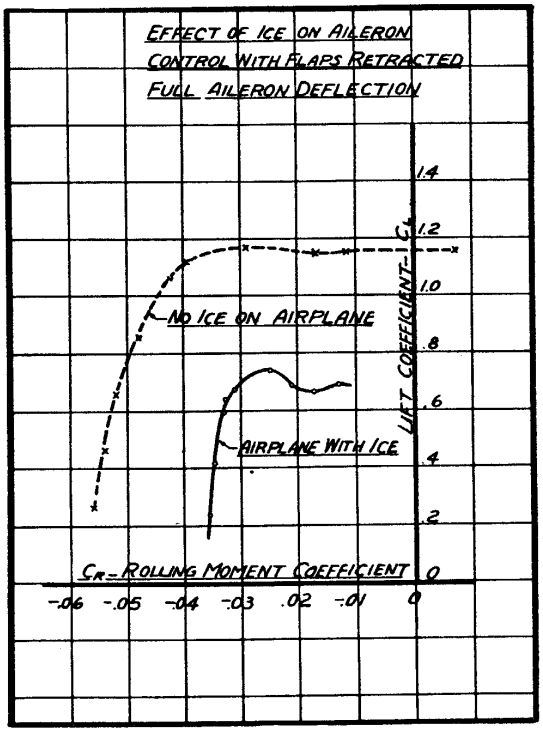

Figure 3. Effect of ice on aileron control[9].

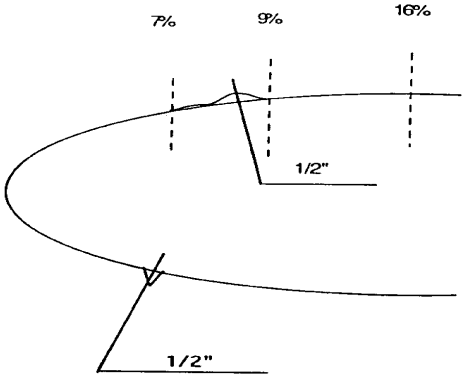

Figure 4. Icing tanker large droplet ice accretion[11]. (180 KIAS, T = -2 C, MVD = 140 microns, LWC = 0.3 g/m^3, 17.5 minutes, and δ_f = 0 deg.)

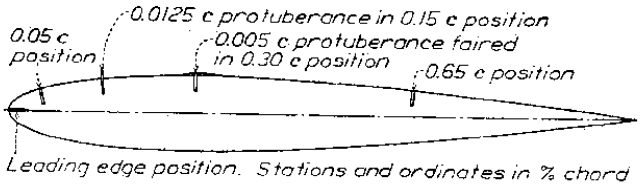

Figure 5. Airfoil and protuberance geometry[13].

a)

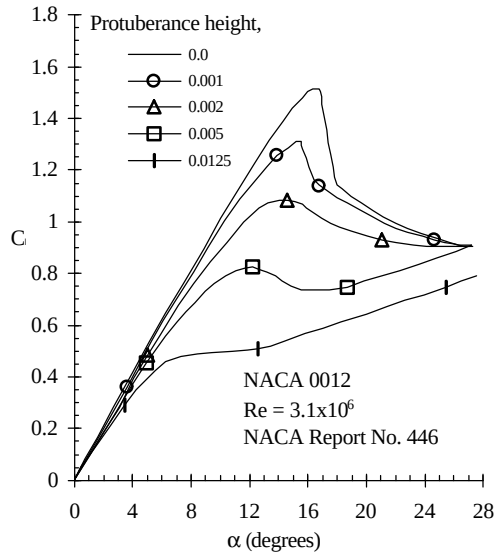

b)

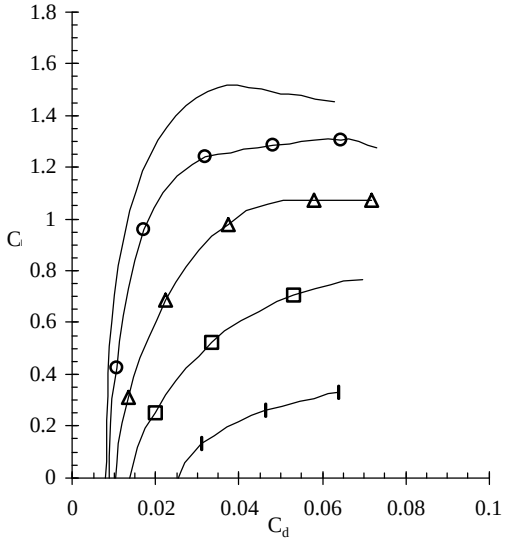

c)

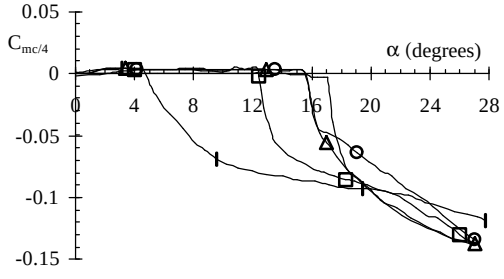

Figure 6. Airfoil performance with protuberance at x/c=0.05 on the upper surface[13].

a)

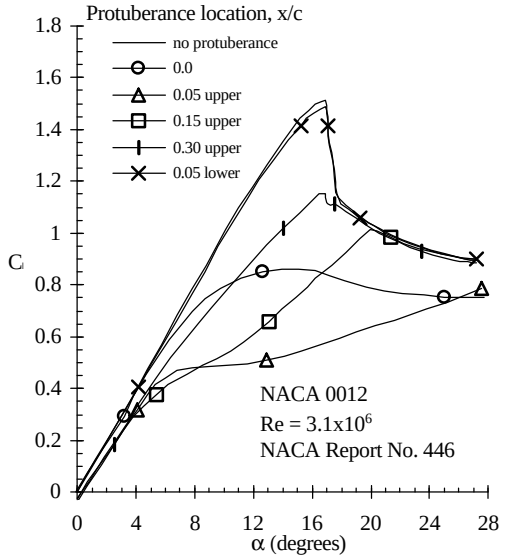

b)

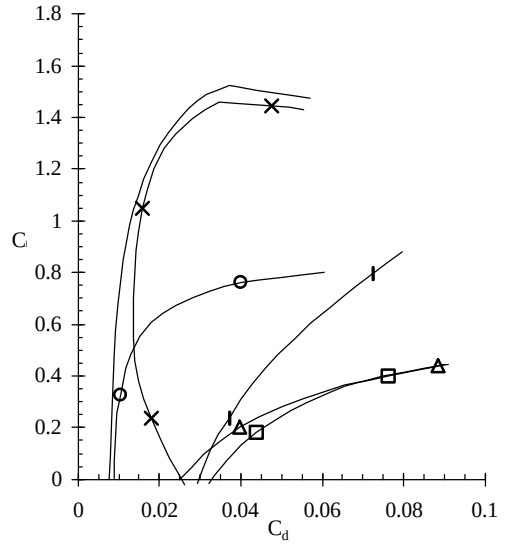

Figure 7. Airfoil performance with 0.0125c protuberance at 5 locations[13].

a)

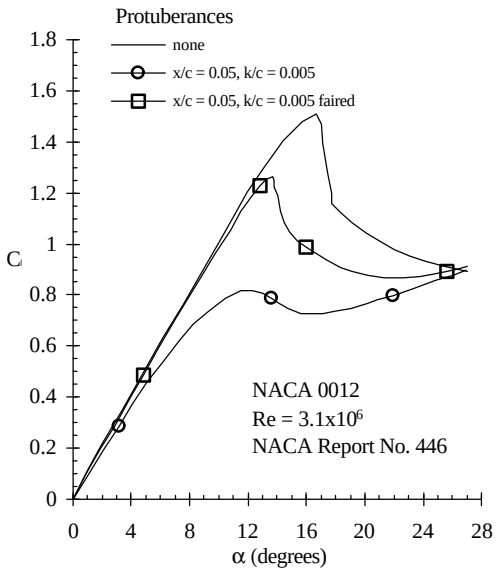

b)

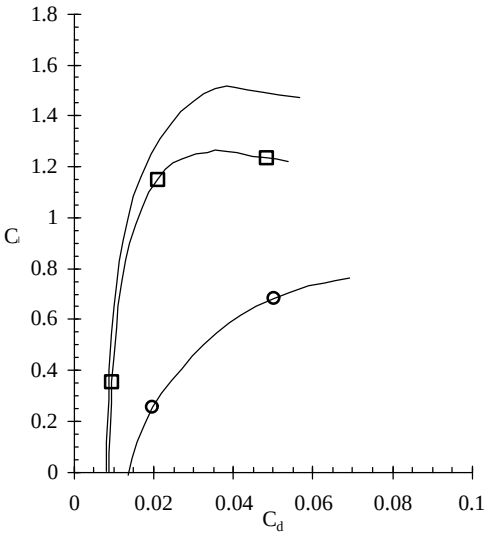

Figure 8. Effect of fairing the 0.005c protuberance at x/c=0.05[13].

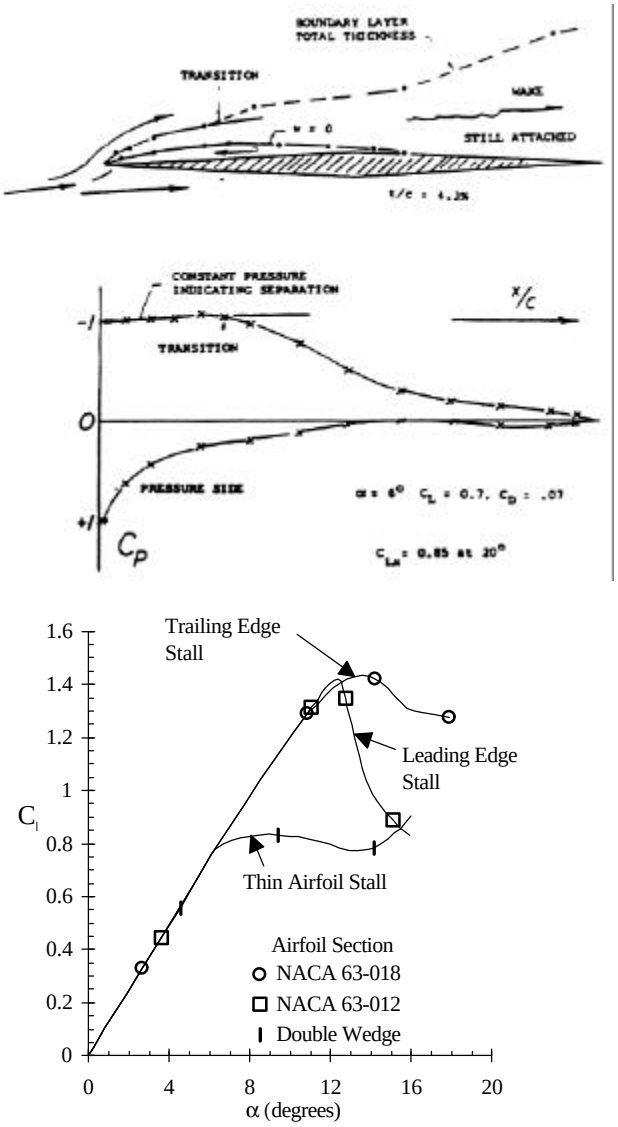

Figure 9. Thin airfoil stall[15,16]. a) diamond airfoil flowfield at stall, b) diamond airfoil Cp at stall, and c) lift of diamond airfoil and other airfoils.

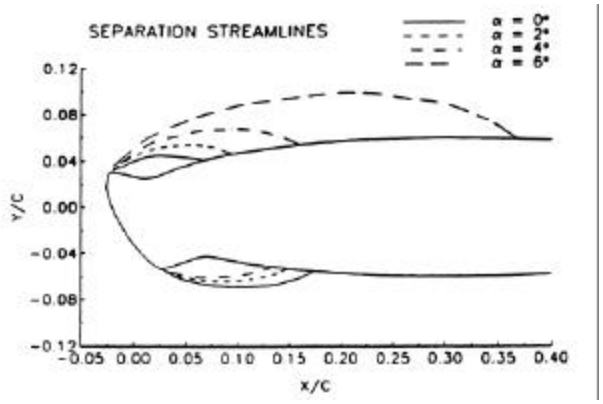

Figure 10. Separation bubble due to a leading-edge ice accretion[18].

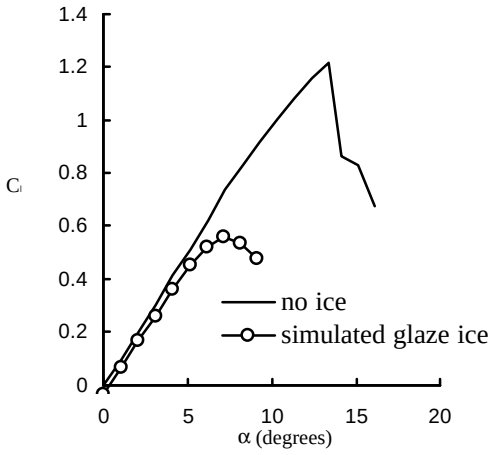

Figure 11. Lift performance of an airfoil with leading-edge ice[18].

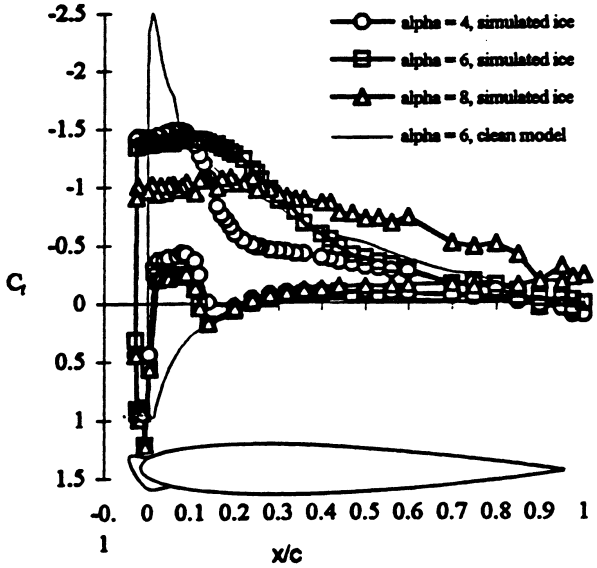

Figure 12. Pressure distribution on an airfoil with leading-edge ice[18].

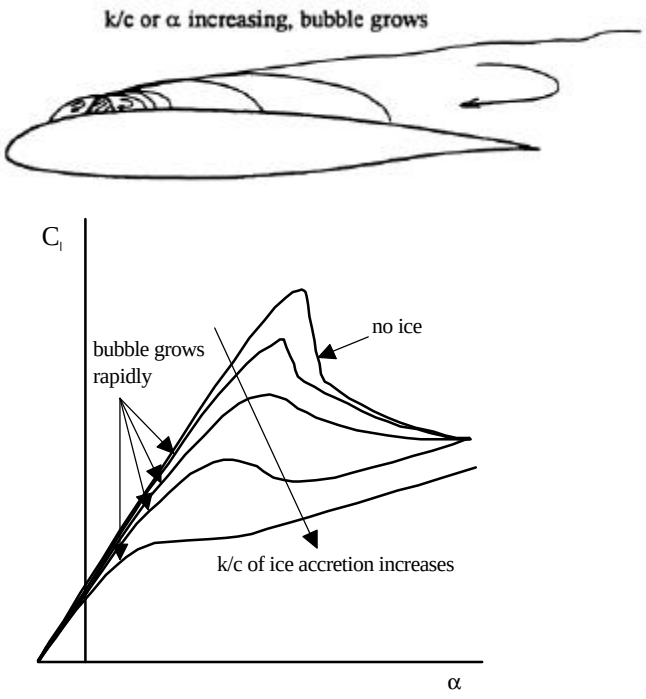

Figure 13. Possible flowfield and lift of an airfoil with a large-droplet ice accretion.

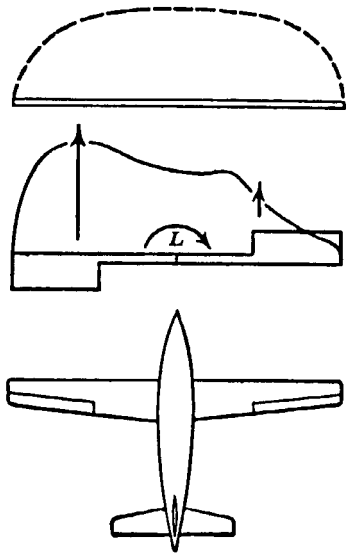

Figure 14. Span load of a wing with aileron deflection[20].

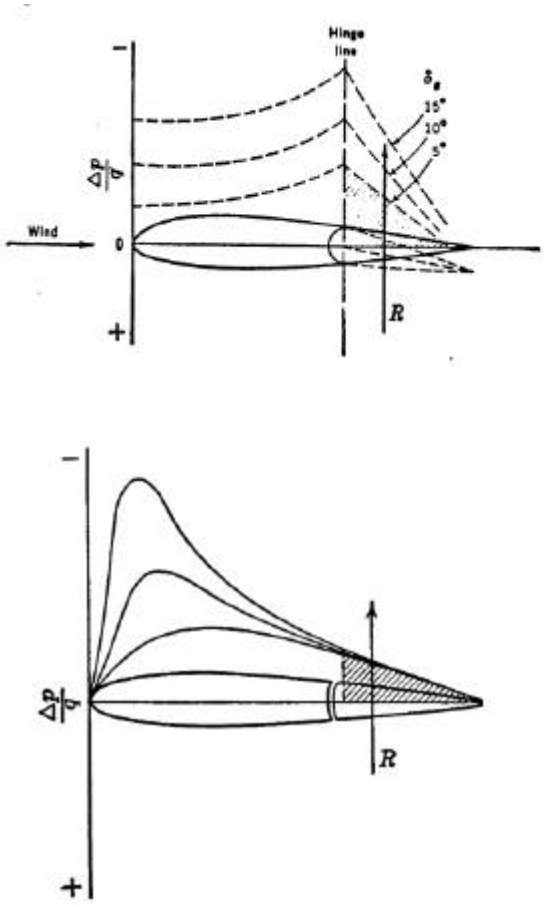

Figure 15. Pressure distribution for an airfoil with aileron deflected[20].

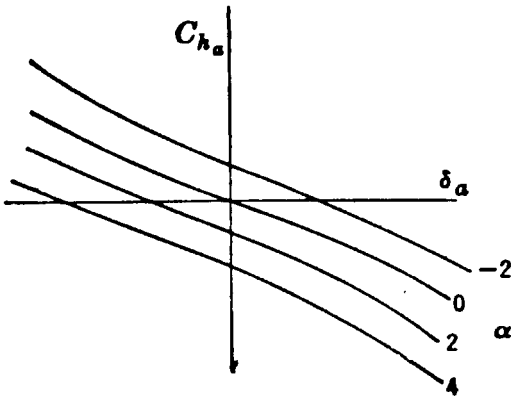

Figure 16. Effect of α and δ_a on hinge moment, C_h[20].

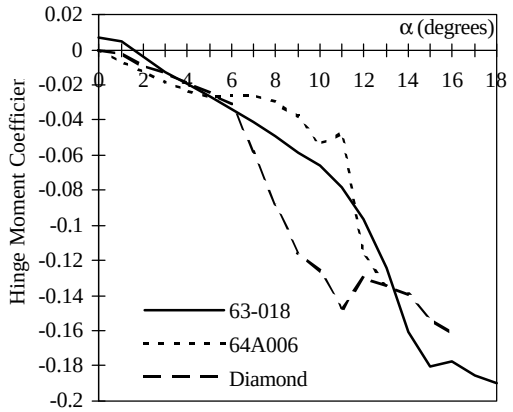

Figure 17. Hinge moments on airfoils with 20% chord plain flaps at δ_f=0. (derived from data in ref. 15)

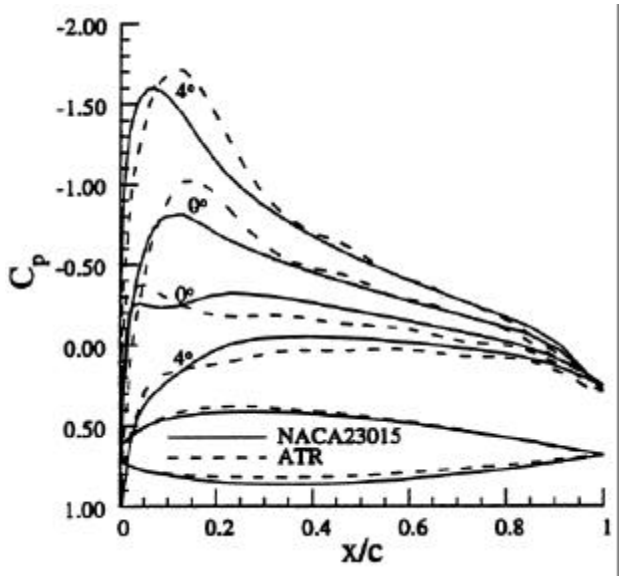

Figure 18. ATR airfoil pressure distribution compared to a NACA 23015.